Desalination and Water Treatment
www.deswater.com
doi: 10.1080/19443994.2014.902337

54 (2015) 2468–2479
May

Taylor & Francis
Taylor & Francis Group

Phosphorus recovery through struvite precipitation from wastewater: effect of the competitive ions

Nancy Y. Acelas[a], Elizabeth Flórez[b], Diana López[a,*]

[a]*Facultad de Ciencias Exactas y Naturales, Química de Recursos Energéticos y Medio Ambiente, Instituto de Química, Universidad de Antioquia, UdeA—Colombia, Calle 70 No. 52-21, Medellín, Colombia, Tel. +57 4 2196613; Fax: +57 4 2191073; email: dplope@gmail.com*
[b]*Departamento de Ciencias Básicas, Universidad de Medellín – Colombia, Carrera 87 No. 30-65, Medellín, Colombia*

Received 13 November 2013; Accepted 1 March 2014

ABSTRACT

In wastewater treatment plants (WWTP), struvite precipitation occurs spontaneously under conditions which are influenced by factors such as: concentration of Mg^{2+}, NH_4^+ and PO_4^{3-}, pH, temperature, and competitive ions. These parameters are often difficult to control and, spontaneous precipitation of struvite creates operational problems in WWTP. Struvite is also a potentially marketable product as a fertilizer alternative. For these two reasons it is important to study the principles of struvite precipitation, and evaluate the parameters that control this process. In this study, the influence of the ions Ca^{2+} and Al^{3+} in struvite precipitation process was evaluated using three different molar ratios of Mg^{2+}:Ca^{2+} and Mg^{2+}:Al^{3+}. The products were characterized by thermogravimetric analysis, X-ray diffraction, and scanning electron micrograph. The results showed that calcium interfered in struvite precipitation only when this is in equal or greater molar ratios to magnesium, while aluminum inhibited completely the production of struvite even at lower aluminum molar ratios to magnesium.

Keywords: Struvite; Wastewater; Phosphorus; Recovery; Precipitation

1. Introduction

Phosphorus (P) is a fundamental element for all living organisms, an essential nutrient for crop production, and there is no substitute for phosphorus in nature [1]. It is mostly obtained from mined rock phosphate and its reserves could be exhausted in the next 50–100 years [2]. On the other hand, phosphorus in wastewater discharged promotes eutrophication of enclosed water bodies such as lakes or harbors [3]. Therefore, it is of great importance to develop a sustainable method to remove and recover phosphorus contained in wastewater [4,5].

The more common methods for phosphorus removal are chemical precipitation and enhanced biological phosphorus removal (EBPR) [6–8]. Chemical precipitation increases sludge volume, decreases the biodegradability of the sludge, and the disposition of the generated sludge is expensive [1]. In the EBPR process, phosphates and other ions (i.e. Mg^{2+}, K^{2+}) are taken up and stored as polyphosphates (Poly-P) inside the bacterial cells. During the anaerobic digestion process, most of the phosphorus stored as Poly-P and part of the phosphorus present in the organic matter

*Corresponding author.

is released to the liquid phase increasing notably the phosphate concentration. Ammonium concentration also increases significantly as proteins are degraded [9–12]. Therefore, the rejected liquors from digested sludge dewatering are very appropriate streams for recovering phosphorus by struvite precipitation [13,14].

The idea of struvite ($MgNH_4PO_4{\cdot}6H_2O$) crystallization in a specific reactor to prevent its spontaneous precipitation has been widely investigated and it has shown great potential as a route for phosphorus recovery in wastewater treatment plants [1,15,16]. Struvite is a white crystalline compound with orthorhombic pattern, composed of magnesium, ammonium, and phosphate. Its composition makes it a potentially marketable product for the fertilizer industry [17,18]. Struvite precipitates in a 1:1:1 M ratio following the general Eq. (1), with $n = 0$, 1, or 2, depending on the solution pH, which regulates the distribution of the various phosphate species [19,20].

$$Mg^{2+} + NH_4^+ + H_nPO_4^{3-n} + 6H_2O \rightarrow MgNH_4PO_4 \cdot 6H_2O + nH^+ \quad (1)$$

The occurrence and development of struvite crystals follows two chemical stages: nucleation (crystal birth) and crystal growth (development of crystals until equilibrium) [19]. Physical–chemical parameters controlling the crystallization process include [20–27]: solution pH, molar ratio (Mg^{2+}:$H_nPO_4^{n-3}$:NH_4^+), temperature, rate of stirring, supersaturation, and presence of foreign ions.

Stratful et al. [21] found that struvite could be precipitated out of solution at pH 10 and the increment of NH_4^+ concentration increased purity of the precipitate. It was also observed that when the reaction time increased from 1 to 180 min, the crystal size increased from 0.1 to 3 mm. Zhang et al. [22] demonstrated that ammonium in landfill leachate is removed as struvite at pH 9.5 and, with the optimal molar ratio Mg^{2+}:NH_4^+:PO_4^{3-} at 1.15:1:1 can remove ammonium effectively and avoid higher concentration of PO_4^{3-} in the effluent. On the other hand, Korchef et al. [20] investigated the precipitation of struvite using the CO_2 degasification technique, the effect of magnesium, phosphate, and ammonium concentrations on the kinetics and the efficiency of struvite precipitation. They found that when increasing the magnesium concentration by keeping constant the phosphate concentration, the phosphate removal efficiency can be significantly improved. However, this improvement led to the co-precipitation with struvite of other magnesium phosphates as well. They also observed that an excess of ammonium in solution favors struvite precipitation.

In addition, it is known that impurities in solution affect the growth rates of crystalline compounds due to blocking of sites where crystals could be formed, inhibiting the increase of crystal size [26,28]. In wastewater effluents where calcium and aluminum levels can be relatively high, these ions can interact with phosphate and affect significantly struvite crystal growth and the characteristics of the produced crystal [29]. It has been observed that a high Ca^{2+}/PO_4^{3-} molar ratio struvite cannot be formed and, it was probably due to the formation of amorphous calcium phosphate [26].

This study explores the effect of the competitive ions such as aluminum and calcium during struvite precipitation and provides a better insight into the dominant compounds formed during the precipitation of struvite as a P-recovery from nutrient-rich wastewater.

2. Materials and methods

2.1. Synthesis of struvite

Synthetic struvite was prepared by mixing equal volumes of two stock solutions with equimolar quantities of Mg^{2+}:PO_4^{3-}:NH_4^+, molar ratio equal to one, which correspond to 27 mg/L Mg^{2+}, 20 mg/L NH_4^+ y 106 mg/L PO_4^{3-}. The first solution was prepared using $MgSO_4{\cdot}7H_2O$ (Sigma–Aldrich > 99%), and the second one by mixing $NaH_2PO_4{\cdot}2H_2O$ (Sigma–Aldrich > 99%) and NH_4Cl (Sigma–Aldrich > 99%). The pH in each solution was adjusted at nine by the addition of sodium hydroxide (NaOH 1M). After that, the stock solutions were mixed and allowed to react during 2 h at 25°C with magnetic stirring (100 rpm). The pH behavior was followed during the reaction, and its evolution with time was then measured. Due to the small quantities of struvite generated it was necessary to increase stoichiometrically the total concentration by factor of seven to allow the formation of measurable amounts of struvite.

2.2. Competitive ions effect

Several batch experiments were carried out to assess the impact of Ca^{2+} and Al^{3+} ions on struvite precipitation. Carbonate is a typical ion found in wastewater, which can compete with phosphate ion during struvite formation and, therefore its effect was evaluated in both solutions. Prior to mix, the solutions

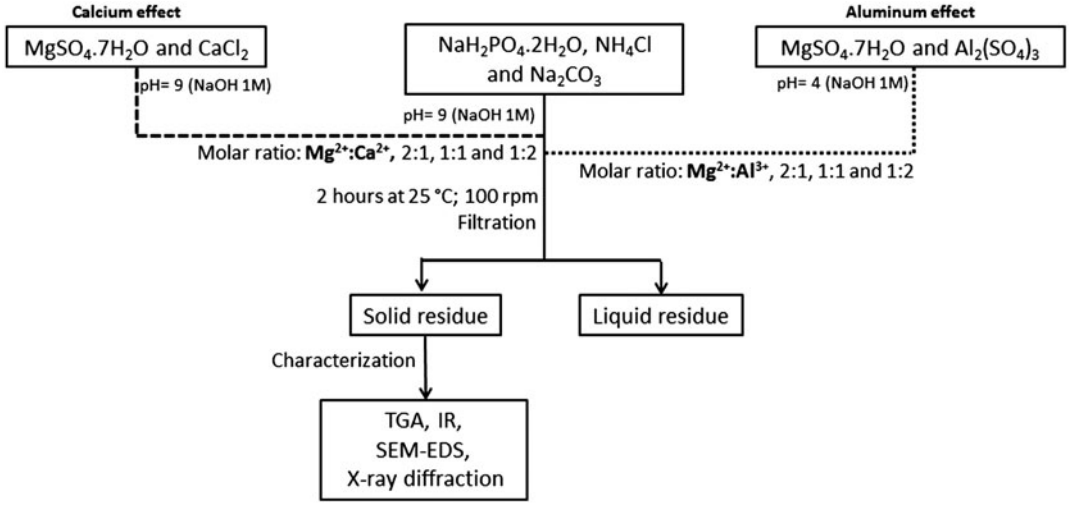

Fig. 1. Experimental diagram of the competitive ion effect during struvite precipitation.

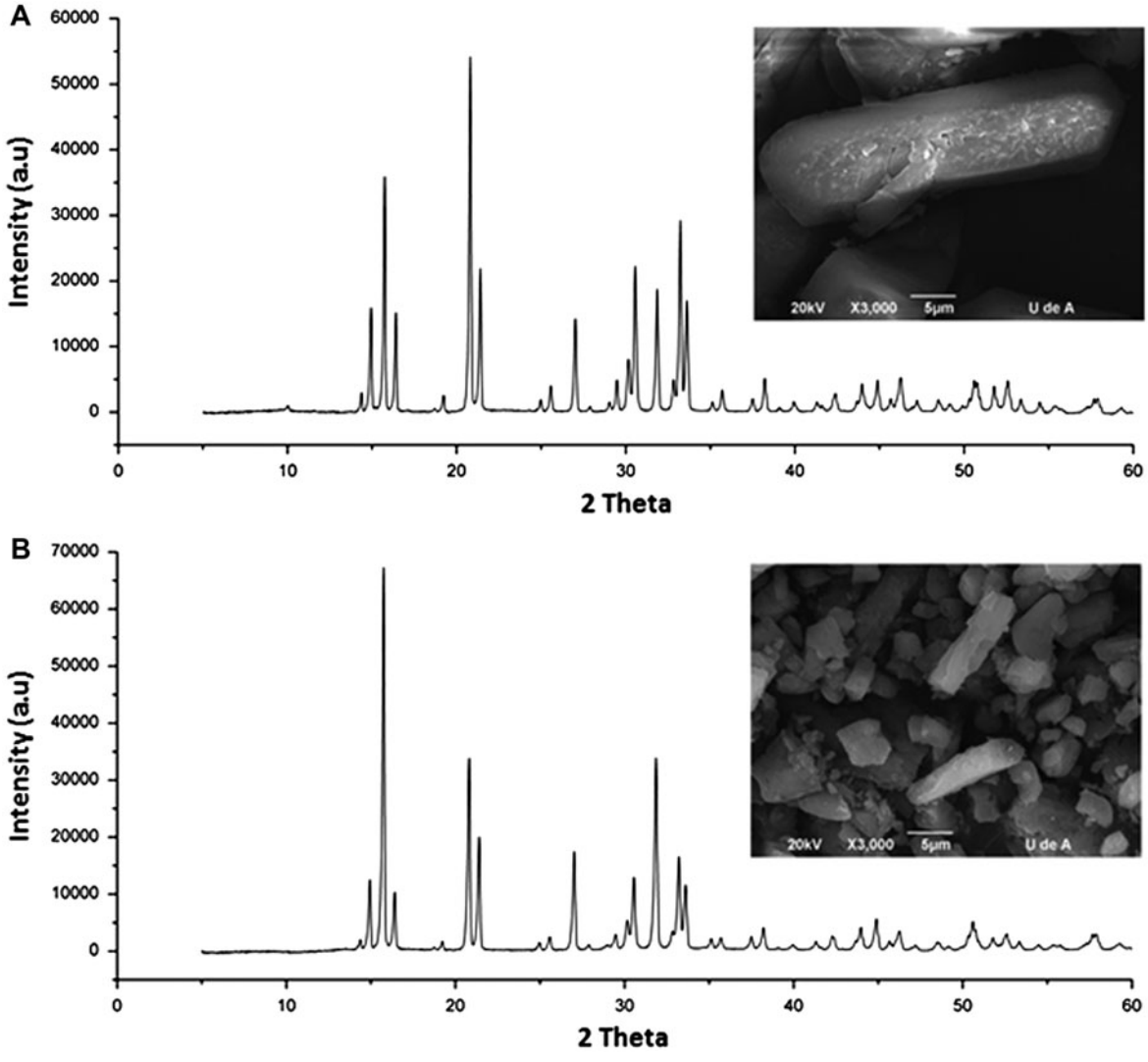

Fig. 2. XRD patterns and SEM micrographs of: (A) reference struvite (Sygma–Aldrich) and (B) synthesized struvite.

to prepare struvite, the $MgSO_4{\cdot}7H_2O$ solution was spiked with Ca^{2+} as $CaCl_2$ (Sigma–Aldrich > 99%) or Al^{3+} as $Al_2(SO_4)_3$ (Sigma–Aldrich > 99%) and the $NaH_2PO_4{\cdot}2H_2O$ and NH_4Cl solution was spiked with CO_3^{2-} as Na_2CO_3 (Sigma–Aldrich > 99%). A total of three solutions were prepared: the first solution containing Mg^{2+} and Ca^{2+}, the second with Mg^{2+} and Al^{3+}, and the third one with PO_4^{3-}, NH_4^+, and CO_3^{2-} ions. During the preparation of the first and the third solution, the pH was adjusted at nine, while the pH for the second solution was maintained at four to allow complete solubilization of the ions in solution (Fig. 1). A molar ratio of 2 for NH_4^+:PO_4^{3-} was used to ensure that this was not a limiting factor on the formation of struvite, and in this case the only limiting factor was the presence of foreign ions.

To evaluate the effect of Ca^{2+} the first solution was added to the third one and, in the case of Al^{3+} the second solution was added to the third one. In both solutions the pH was adjusted at nine using NaOH 0.1M. The molar ratios Mg^{2+}:Ca^{2+}:CO_3^{2-} and Mg^{2+}:Al^{3+}:CO_3^{2-} investigated here were 2:1:1, 1:1:1, and 1:2:2.

2.3. Product characterization

At the end of each test, the precipitated solid was filtrated through 0.22 μm filters, dried at 105°C for 24 h until constant weight and then characterized using thermogravimetric analysis (TGA) (TGA Q500), room temperature infrared (IR) spectra in the wave number range of 400–4,000 cm^{-1} (Perkin Elmer 1710), X-ray diffraction (XRD) (Powder X-ray Diffractometer D5005 Siemens), and SEM–EDS (Philips XL 30 SFEG).

3. Results and discussion

It has been reported that in sludge liquors, where calcium levels can be relatively high, the magnesium to calcium ratio (Mg^{2+}:Ca^{2+}) ranging from 1:1.4 to 1:3.7 can affect the struvite precipitation process [19]. Although to the knowledge of the authors there have not been reports about the influence of the aluminum on struvite crystallization, it is possible to infer that according to the cationic nature of the aluminum it could react with phosphate anion and affects negatively the occurrence of struvite crystals. The given information above was used to define the molar ratio of the competitive cations evaluated in this study.

3.1. Identification of struvite

An indication of struvite nucleation is the pH. According to Eq. (1), during struvite formation, proton ions are released into solution which results in a decrease in pH. The drop in pH is characteristic of the rate at which the first crystals of struvite occur and is linked to the rate of struvite formation, which can influence the quality of the crystals formed. During the first 30 min of reaction it was possible to observe the decrease of the pH solution from 9 to 6 and, then the pH was constant with a value of 5, which means that the struvite formation ended.

Fig. 2 shows that the powdered XRD pattern of reference (Sygma–Aldrich) and synthesized struvite matched very well and, the orthorhombic pattern observed in the scanning electron micrograph (SEM) for both samples is consistent with the morphology reported for this compound [20]. Therefore, the

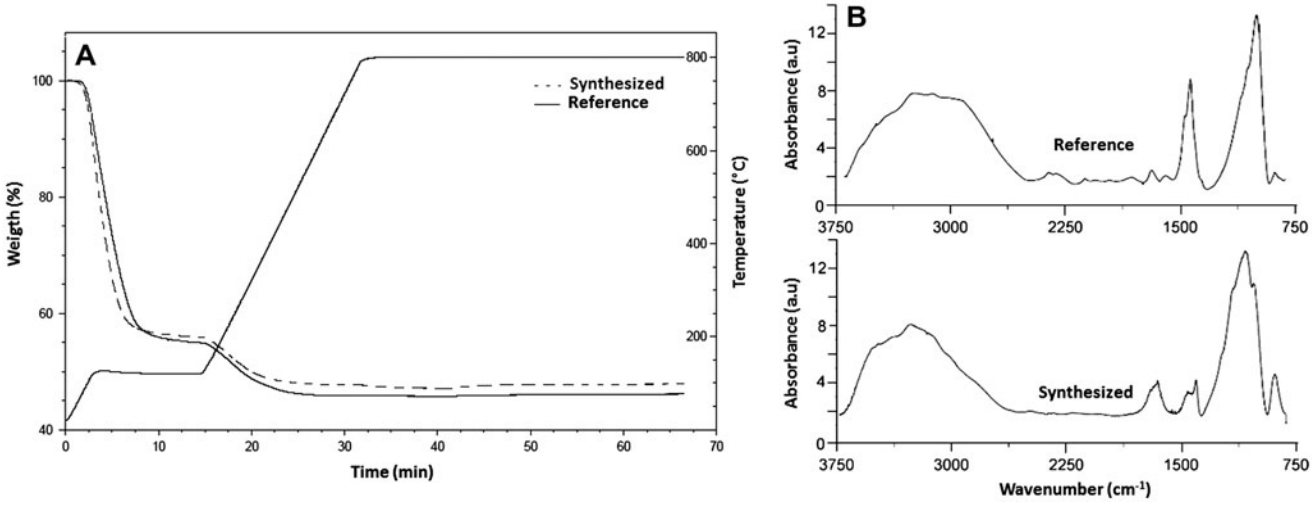

Fig. 3. (A) Thermogravimetric and (B) IR analysis for reference struvite (Sygma–Aldrich) and synthesized struvite.

synthesis method used in this study is suitable for the production of struvite. Additionally, Fig. 3 shows the TGA curves for reference and synthesized struvite. These data indicate that mass loss begins at temperature around 100°C and is essentially complete when the temperature reached above 250°C. At this point, 51% of the original mass loss occurred. This mass loss corresponds to the following decomposition reaction for struvite, Eq. (2):

$$MgNH_4PO_4.6H_2O \rightarrow MgHPO_4 + 6H_2O\uparrow + NH_3\uparrow \quad (2)$$

According to TGA results the first loss of mass is 44.19 and 44.10% and the second one is 7.69 and 7.54% for the reference and synthesized struvite, respectively. These results are in agreement with the theoretical mass loss for the formula ($NH_4MgPO_4{\cdot}6H_2O$) which is 51.42% which is made up of mass loss of water as 44.08% and ammonia as 7.34%. It is possible to observe the same behavior for both samples which confirms the identity of the synthesized struvite. Infrared spectra (Fig. 3(B)) for both reference and synthesized struvite show a set of bands at 1,675, 1,591, and 1,440 cm^{-1}. The first band is assigned to HOH water deformation and, the following two bands to the deformation modes of HNH from NH_4 units. Bands at 980 and 1,065 cm^{-1} are assigned to antisymmetric vibration modes of PO_4, the band found at 3,400 cm^{-1} is attributed to OH stretching of water and, the band at 748 cm^{-1} is attributed to the oscillation modes of NH_4. The correspondence between the IR spectra of synthesized and reference

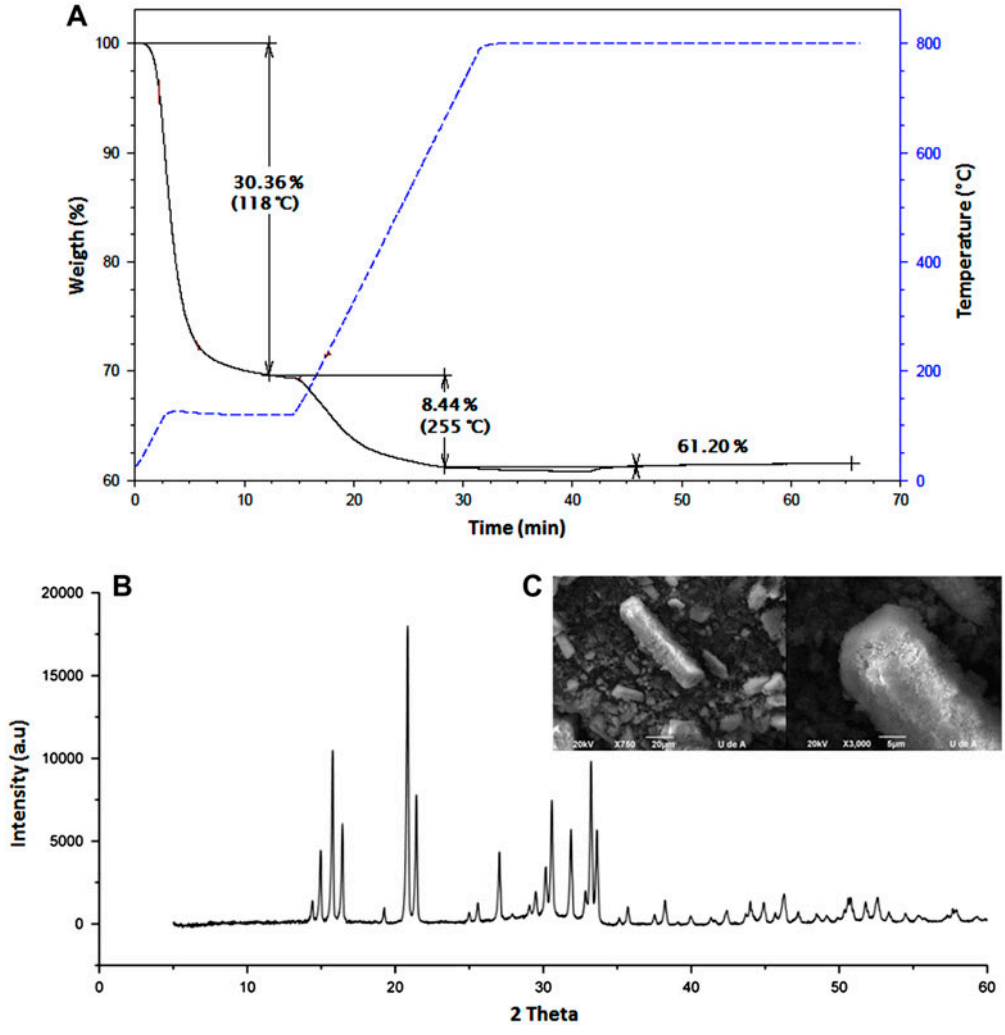

Fig. 4. Calcium ions effect in struvite precipitation. (A) TGA, (B) XRD patterns, and (C) SEM micrographs for the molar ratio 2:1, Mg^{2+}:Ca^{2+}.

struvite corroborates the formation of this compound with the proposed methodology.

3.2. Effect of calcium and aluminum concentration on struvite precipitation.

3.2.1. Molar ratio 2:1 Mg^{2+}:Ca^{2+} and Mg^{2+}:Al^{3+}

Fig. 4(A) shows the TGA for the solid obtained using a molar ratio of 2:1 Mg^{2+}:Ca^{2+}. A similar thermogram was obtained in comparison with the reported for synthesized struvite, i.e. with three mass losses using calcium like competitive ion. However, there are differences in the amount of each mass loss with a remarkable increase of the residue, which suggests the formation of other compounds with struvite. According to the experimental conditions, Ca^{2+} ions effectively interact with phosphate or carbonate ions to form calcium phosphate (hydroxyapatite) (Eq. (3)) or calcium carbonate (Eq. (4)), which are not able to inhibit the struvite formation, but are part of the impurities of this compound.

$$5Ca^{2+} + 3PO_4^{3-} + H_2O \rightarrow Ca_5(PO_4)_3OH + H^+ \quad (3)$$

$$Ca^{2+} + CO_3^{2-} \rightarrow CaCO_3 \quad (4)$$

Fig. 4(B) and (C) shows the XRD pattern and SEM micrograph for the solid obtained for the molar ratio 2:1 Mg^{2+}:Ca^{2+}. It can be identified the diffraction pattern for struvite and, its orthorhombic morphology.

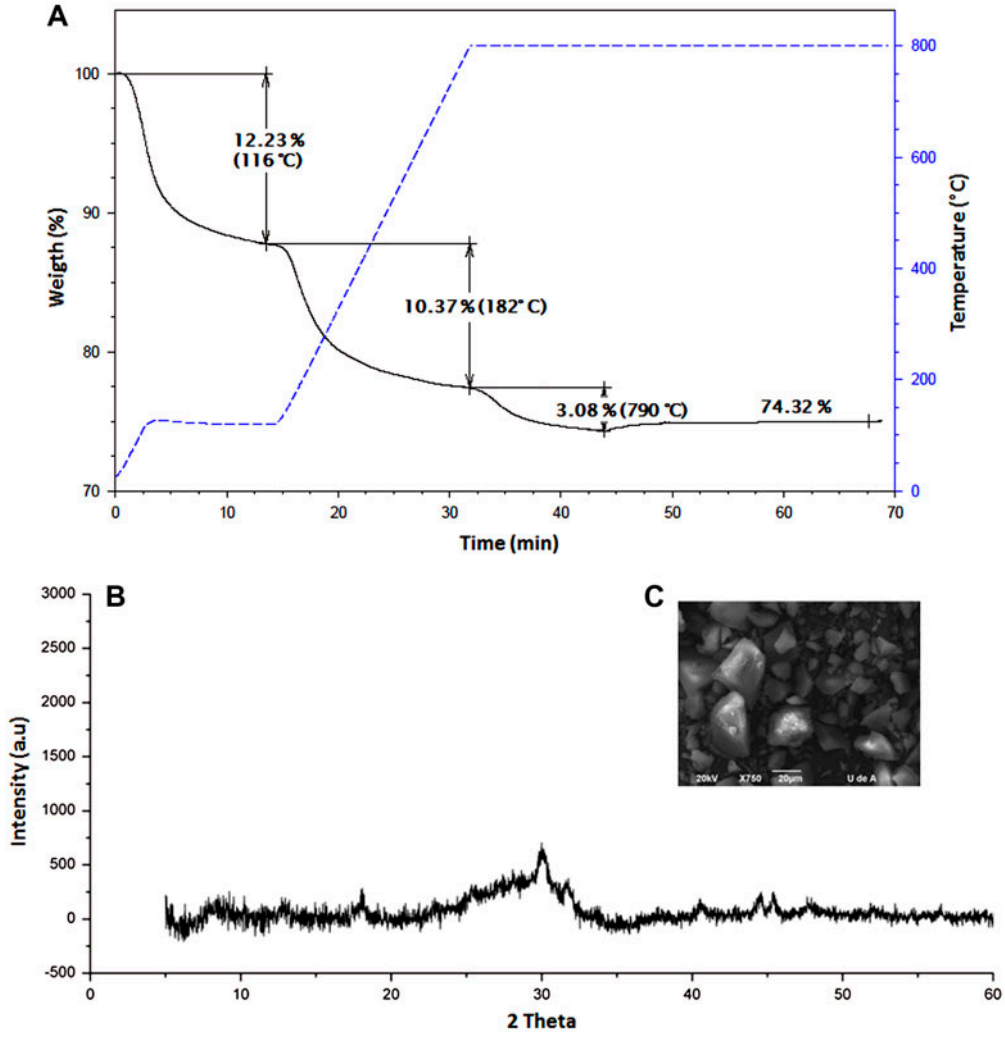

Fig. 5. Aluminum ions effect in struvite precipitation. (A) TGA, (B) XRD patterns, and (C) SEM micrographs for the molar ratio 2:1, Mg^{2+}:Al^{3+}.

Table 1
Main reactions during the thermal decomposition of the compounds in the solid

Reaction		Decomposition temperature (°C)
$CaCO_{3(s)} \rightarrow CaO_{(s)} + CO_{2(g)}$	(5)	600–850
$MgCO_{3(s)} \rightarrow MgO_{(s)} + CO_{2(g)}$	(6)	480
$Mg(OH)_{2(s)} \rightarrow MgO_{(s)} + H_2O_{(g)}$	(7)	300–450
$Ca(OH)_{2(s)} \rightarrow CaO_{(s)} + H_2O_{(g)}$	(8)	340–480
$Ca_3(PO_4)_{2(s)} \rightarrow$ Estable	(9)	Stable at high T
$Ca_9(PO_4)_6.OH_{(s)} \rightarrow Ca_9(PO_4)_{6(s)} + OH_{(g)}$	(10)	1,000–1,450
$Mg_3(PO_4)_2.8OH_{(s)} \rightarrow Mg_3(PO_4)_{2(s)} + 8OH_{(g)}$	(11)	250
$MgHPO_{4(s)} \rightarrow Mg_2P_2O_{7(s)}$	(12)	> 800
$2Al(OH)_{3(s)} \rightarrow Al_2O_{3(s)} + 3H_2O_{(g)}$	(13)	272–300
$Al_2(SO_4)_{3(s)} \rightarrow Al_2O_{3(s)} + 3SO_{3(g)}$	(14)	> 700
$AlPO_4.1.5H_2O_{(s)} \rightarrow AlPO_{4(s)} + 1.5H_2O_{(g)}$	(15)	400
$MgSO_{4(s)} \rightarrow MgO_{(s)} + SO_{3(g)}$	(16)	> 800

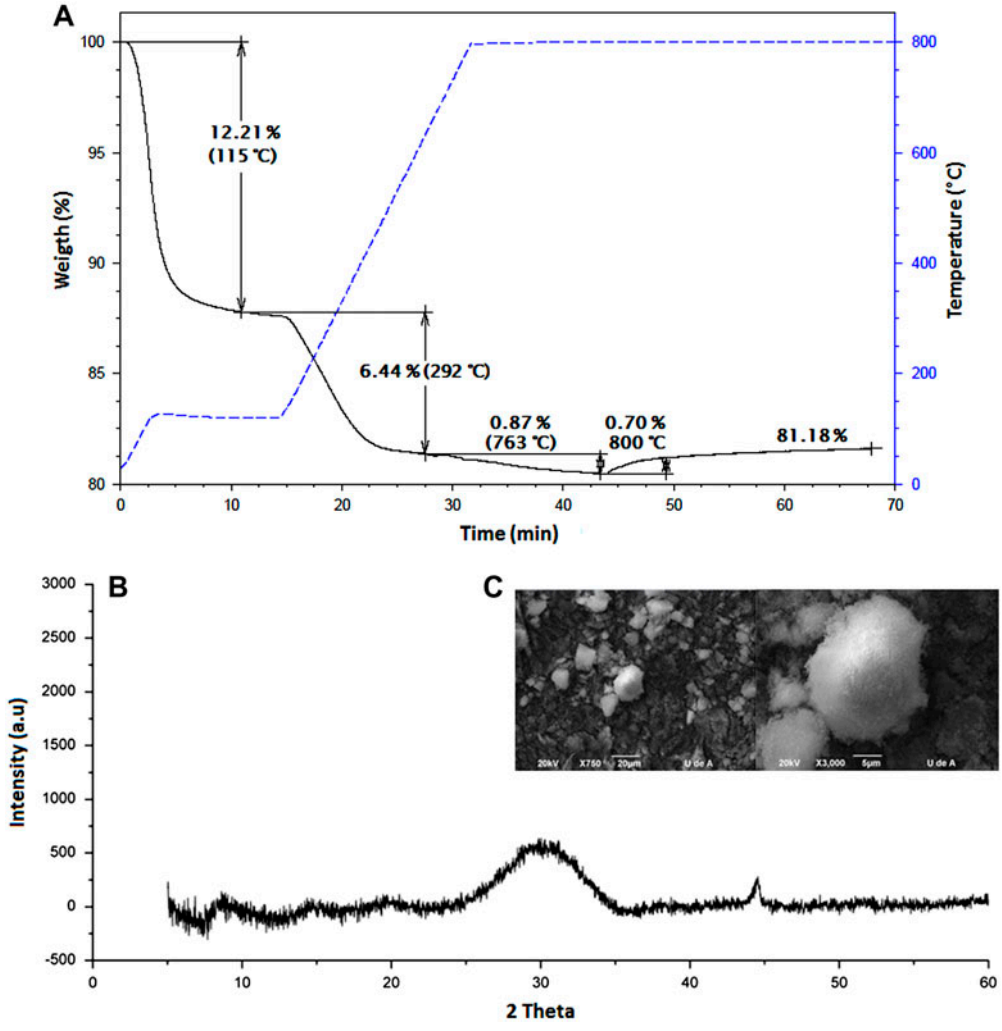

Fig. 6. Calcium ions effect in struvite precipitation. (A) TGA, (B) XRD patterns, and (C) SEM micrographs for the molar ratio 1:2, Mg^{2+}:Ca^{2+}.

Similarly, an amorphous solid over the orthorhombic crystals is observed, which could correspond to calcium carbonate or calcium phosphate or a mixture of these two compounds. Therefore, with a molar ratio 2:1 of Mg^{2+}:Ca^{2+} is still possible to obtain struvite. A possible explanation of struvite nucleation under these conditions is that phosphate ions are in excess in comparison to calcium ions and, even if all calcium reacts preferentially with phosphate to form calcium phosphate, the minimum ratio 1:1:1 Mg^{2+}:NH_4^+:PO_4^{3-} necessary for struvite formation, is still available. At this ratio, calcium ions affect growth rate and induction time in crystals formation, but not the compound formation [30].

For the molar ratio 2:1 of Mg^{2+}:Al^{3+}, the TGA (Fig. 5(A)) shows a different pattern, therefore under these conditions it was not possible to form struvite. The effect of Al^{3+} ion in struvite precipitation was more drastic than the effect of Ca^{2+} ion, with zero probability in the formation of this compound. The diffraction pattern and SEM micrograph are shown in Fig. 5(B) and (C). It can be observed that the solid of this experiment does not have a diffraction pattern and, also the orthorhombic morphology is completely lost. These results are in agreement to the TGA.

3.2.2. Molar ratio 1:2 and 1:1. Mg^{2+}:Ca^{2+}

TGA using the molar ratio 1:2 and 1:1 Mg^{2+}:Ca^{2+} is presented in Figs. 6(A) and 7(A), respectively. It can be seen three mass losses, which indicated that if struvite was formed, it was not completely pure. In these experiments, there are conditions to form different types of compounds like, calcium and magnesium

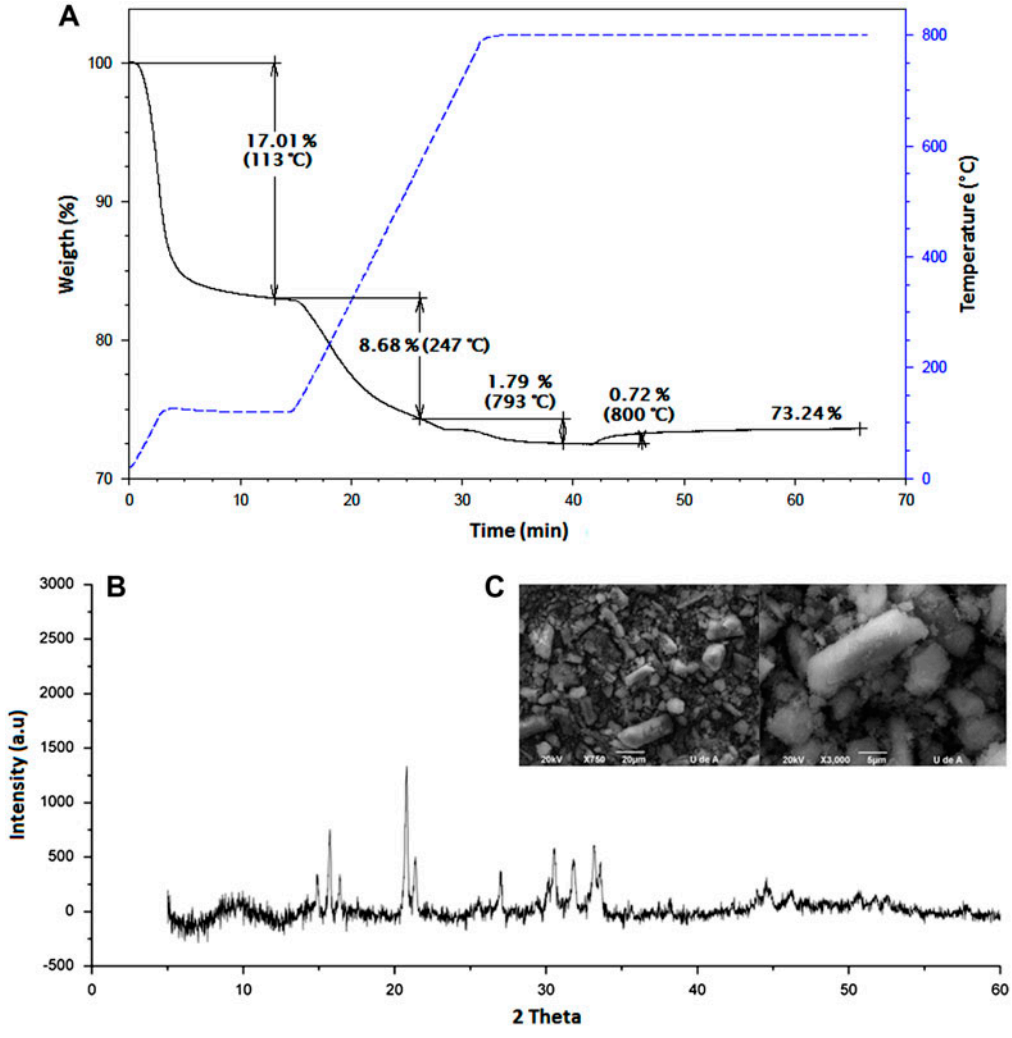

Fig. 7. Calcium ions effect in struvite precipitation. (A) TGA, (B) XRD patterns and (C) SEM micrographs for the molar ratio 1:1, Mg^{2+}:Ca^{2+}.

carbonates, phosphates, and hydroxides. Thus, the first mass loss could be associated to the surface moisture, the second one associated to carbonates decomposition and the evolution of hydration water and, the third one associated to the total oxidation of such compounds.

Table 1 presents the reactions and their decomposition temperatures for the formed compounds (Eqs. (5)–(12)). According to the evolution profile in thermogram (Fig. 6(A)) and, the decomposition temperature for $MgCO_{3(s)}$, $Mg(OH)_2$, and $Ca(OH)_2$ the second mass loss of 6.44% corresponds to the decomposition of these compounds. Similarly, the decomposition temperature of $CaCO_{3(s)}$ (600–900˚C) [31,32], indicates that the formation of this compound was in less proportion when the molar ratio Mg^{2+}:Ca^{2+}, was 1:2 than when the molar ratio Mg^{2+}:Ca^{2+} was 1:1, with a weight loss of 0.87 and 1.79%, respectively. The high residue amount 81.18 and 73.24% for the molar ratio Mg^{2+}:Ca^{2+}, 1:2 and 1:1, respectively, correspond to the decomposition of the compound mentioned above and, also to the formation of calcium phosphate ($Ca_3(PO_4)_2$ o $Ca_9(PO_4)_6$.OH), and $Mg_2P_2O_7$ which are thermally stable in the studied temperature range. XRD analysis (Figs. 6(B) and 7(B)) show a noisy diffraction pattern, however, when the molar ratio Mg^{2+}:Ca^{2+} was 1:1 it was possible to identify some signals which could correspond to struvite, while when the

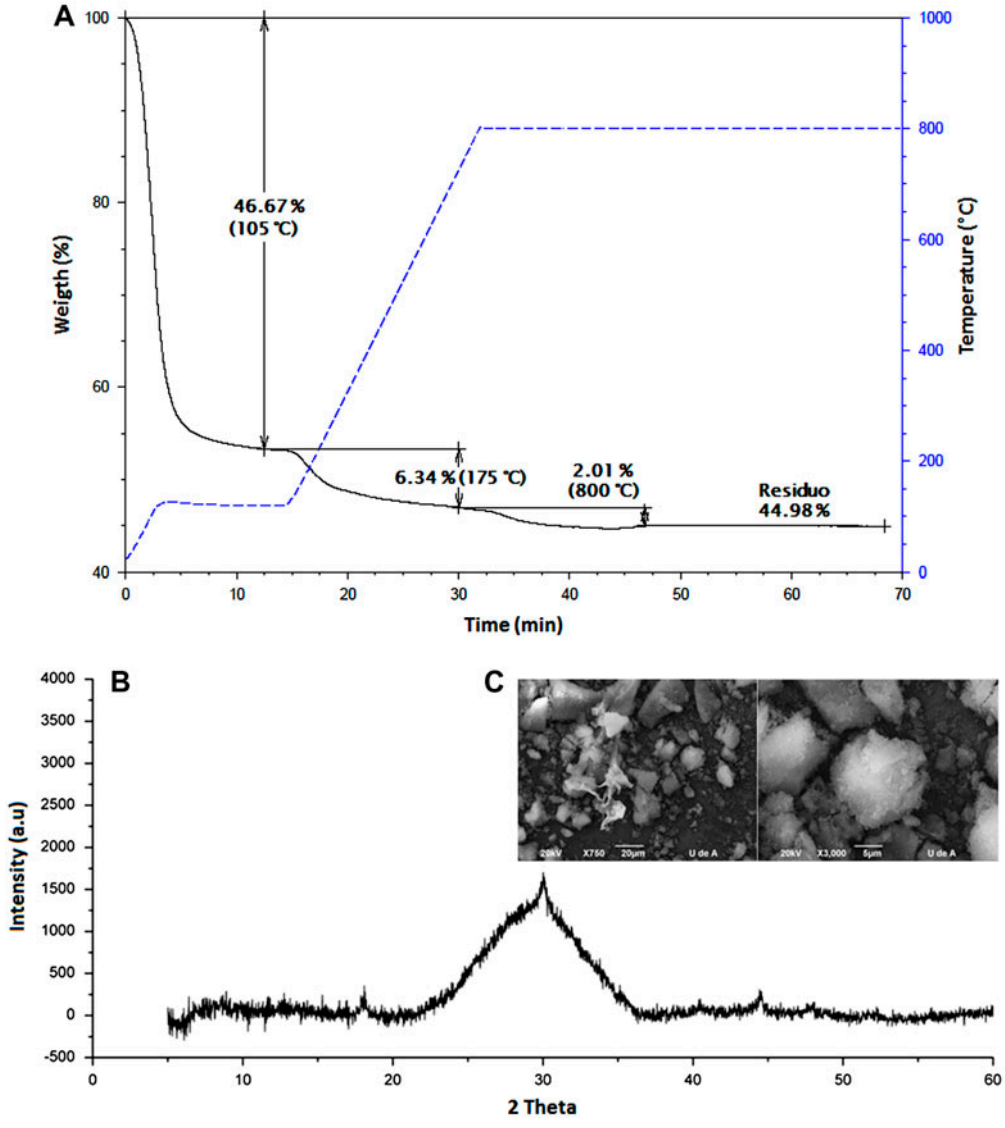

Fig. 8. Aluminum ions effect in struvite precipitation. (A) TGA, (B) XRD patterns, and (C) SEM micrographs for the molar ratio 1:2, Mg^{2+}:Al^{3+}.

ratio Mg^{2+}:Ca^{2+} was 1:2, there was not a defined diffraction pattern. Thus, as calcium concentration increased, the struvite formation is inhibited, which lead to the formation of amorphous material. SEM micrographs show an amorphous material (Fig. 6(C)) and, another with an orthorhombic distorted geometry (Fig. 7(C)). These observations help to corroborate the findings from the TGA.

3.2.3. Molar ratio 1:2 and 1:1. Mg^{2+}:Al^{3+}

TGA which shows the effect of aluminum in struvite precipitation with the molar ratio Mg^{2+}:Al^{3+}, 1:2 and 1:1 are shown in Figs. 8(A) and 9(A), respectively. The profiles of these thermograms show three mass losses. The first one corresponds to moisture loss, the second one is associated with the decomposition of $MgCO_{3(s)}$, $Mg(OH)_2$, and $Al(OH)_3$, and the third loss corresponds to the decomposition of $Al_2(SO_4)_3$ and $MgSO_4$, reactions 14 and 16, Table 1, respectively. The residue in the analyzed solids was around of 84% (dry basis), consisting mainly of the decomposition products of the above compounds (i.e. Al_2O_3 and MgO), and stable phosphates at high temperatures. The XRD and SEM analyses (Figs. 8 and 9(B)–(C)), show that the compounds formed under these experimental parameters are amorphous and without any diffraction pattern, which confirms that there was not stru-

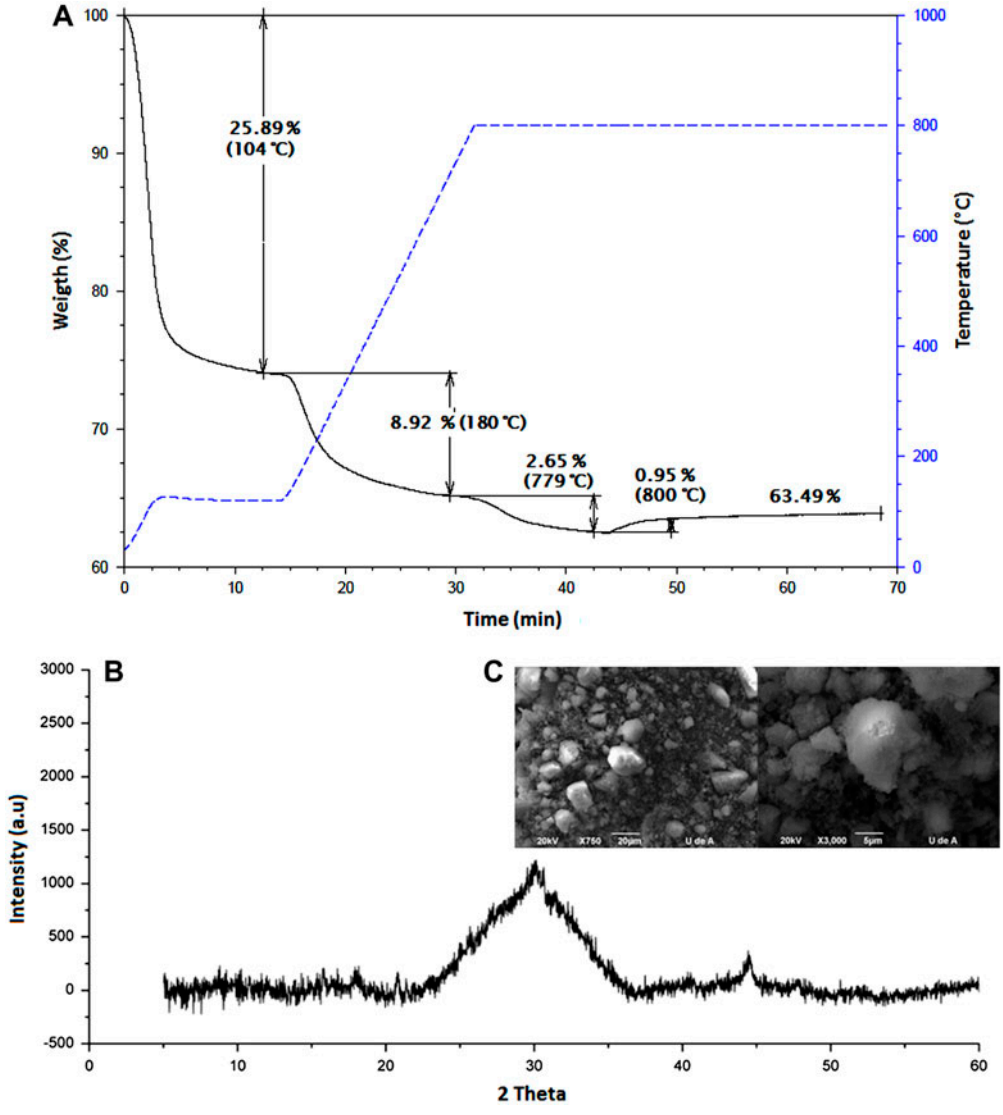

Fig. 9. Aluminum ions effect in struvite precipitation. (A) TGA, (B) XRD patterns, and (C) SEM micrographs for the molar ratio 1:1, Mg^{2+}:Al^{3+}.

vite formation, and the aluminum ion competes efficiently with magnesium to the formation of amorphous phosphate.

Thus, the struvite formation can be interfered by reducing the concentration of any three principal ions that form this compound, Mg^{2+}, NH_4^+, or PO_4^{3-}. In this case, this reduction is through the complexation of orthophosphate ions with a trivalent metal (Al^{3+}). Precipitation of aluminum orthophosphate (Eq. (5)), decreases the amount of soluble phosphorus in wastewater and, therefore the potential for struvite crystallization is reduced.

$$Al^{3+} + PO_4^{3-} \rightarrow AlPO_{4(s)} \quad (5)$$

The results of this study are in agreement with some reports, authors argue that in the case of calcium the interference in struvite crystallization, is due to the formation of insoluble calcium phosphates [28,33–35]. In general, the precipitation process for the different kinds of solids detected, amorphous calcium, magnesium and aluminum phosphate, and struvite was probably a result of kinetics of the reactions. The kinetics of these compounds is influenced by the concentration of magnesium and orthophosphates in the liquid phase. Struvite precipitation is a first rate reaction regarding supersaturation [36] thus, increases of magnesium in the liquid phase benefit the struvite precipitation. Moreover, the crystallization reaction rate is also influenced by the available crystal area, this means by the presence of struvite. This might explain why during the experiments with aluminum, the struvite disappeared in the solid phase even at higher molar ratio of Mg^{2+}:Al^{3+}, 2:1.

4. Conclusions

This study showed that calcium and aluminum ions have a significant impact on the process of struvite precipitation. Increasing the concentration of calcium, the nucleation struvite process decreased. For the molar ratio Mg^{2+}:Ca^{2+}, 2:1 it was possible to find struvite crystals, with the presence of an amorphous precipitate, whereas for the molar ratio Mg^{2+}:Ca^{2+}, 1:2 the struvite formation was completely inhibited and, amorphous compounds were formed. In the case of aluminum, this cation completely inhibited struvite formation, which is associated with high capacity of Al^{3+} to form phosphates. Due to the high concentrations of calcium and aluminum commonly found in wastewater, the impact on the crystal morphology and the inhibition of the process of struvite precipitation should be taken into account in order to improve the recovery and reuse of phosphorus as fertilizer.

Acknowledgments

The authors are grateful to EPM/CIIEN and COLCIENCIAS for financing the project 1115-4547-21979, and to the University of Antioquia for the financial support of the "Programa Sostenibilidad 2013-2014." NA thanks "COLCIENCIAS" and the University of Antioquia for the PhD scholarship.

References

[1] L. Shu, P. Schneider, V. Jegatheesan, J. Johnson, An economic evaluation of phosphorus recovery as struvite from digester supernatant, Bioresour. Technol. 97 (2006) 2211–2216.
[2] D. Cordell, J.-O. Drangert, S. White, The story of phosphorus: Global food security and food for thought, Global Environ. Change 19 (2009) 292–305.
[3] M.R. Awual, A. Jyo, T. Ihara, N. Seko, M. Tamada, K.T. Lim, Enhanced trace phosphate removal from water by zirconium(IV) loaded fibrous adsorbent, Water Res. 45 (2011) 4592–4600.
[4] H. Xu, P. He, W. Gu, G. Wang, L. Shao, Recovery of phosphorus as struvite from sewage sludge ash, J. Environ. Sci. 24 (2012) 1533–1538.
[5] N.Y. Acelas, S.M. Mejia, F. Mondragón, E. Flórez, Density functional theory characterization of phosphate and sulfate adsorption on Fe-(hydr)oxide: Reactivity, pH effect, estimation of Gibbs free energies, and topological analysis of hydrogen bonds, Comput. Theor. Chem. 1005 (2013) 16–24.
[6] M.F.R. Zuthi, W.S. Guo, H.H. Ngo, L.D. Nghiem, F.I. Hai, Enhanced biological phosphorus removal and its modeling for the activated sludge and membrane bioreactor processes, Bioresour. Technol. 139 (2013) 363–374.
[7] A. Oehmen, P.C. Lemos, G. Carvalho, Z. Yuan, J. Keller, L.L. Blackall, M.A.M. Reis, Advances in enhanced biological phosphorus removal: From micro to macro scale, Water Res. 41 (2007) 2271–2300.
[8] A.H. Caravelli, C. De Gregorio, N.E. Zaritzky, Effect of operating conditions on the chemical phosphorus removal using ferric chloride by evaluating orthophosphate precipitation and sedimentation of formed precipitates in batch and continuous systems, Chem. Eng. J. 209 (2012) 469–477.
[9] D. Wild, A. Kisliakova, H. Siegrist, Prediction of recycle phosphorus loads from anaerobic digestion, Water Res. 31 (1997) 2300–2308.
[10] Z. Yuan, S. Pratt, D.J. Batstone, Phosphorus recovery from wastewater through microbial processes, Curr. Opin. Biotechnol. 23 (2012) 878–883.
[11] L. Stante, C.M. Cellamare, F. Malaspina, G. Bortone, A. Tilche, Biological phosphorus removal by pure culture of Lampropedia spp, Water Res. 31 (1997) 1317–1324.
[12] R. Yu, J. Geng, H. Ren, Y. Wang, K. Xu, Combination of struvite pyrolysate recycling with mixed-base technology for removing ammonium from fertilizer wastewater, Bioresour. Technol. 124 (2012) 292–298.

[13] N. Martí, L. Pastor, A. Bouzas, J. Ferrer, A. Seco, Phosphorus recovery by struvite crystallization in WWTPs: Influence of the sludge treatment line operation, Water Res. 44 (2010) 2371–2379.
[14] L. Pastor, N. Marti, A. Bouzas, A. Seco, Sewage sludge management for phosphorus recovery as struvite in EBPR wastewater treatment plants, Bioresour. Technol. 99 (2008) 4817–4824.
[15] E.V. Münch, K. Barr, Controlled struvite crystallisation for removing phosphorus from anaerobic digester sidestreams, Water Res. 35 (2001) 151–159.
[16] H. Huang, C. Xu, W. Zhang, Removal of nutrients from piggery wastewater using struvite precipitation and pyrogenation technology, Bioresour. Technol. 102 (2011) 2523–2528.
[17] K.S. Le Corre, E. Valsami-Jones, P. Hobbs, B. Jefferson, S.A. Parsons, Agglomeration of struvite crystals, Water Res. 41 (2007) 419–425.
[18] R. Yu, J. Geng, H. Ren, Y. Wang, K. Xu, Struvite pyrolysate recycling combined with dry pyrolysis for ammonium removal from wastewater, Bioresour. Technol. 132 (2013) 154–159.
[19] K.S. Le Corre, E. Valsami-Jones, P. Hobbs, S.A. Parsons, Phosphorus recovery from wastewater by struvite crystallization: A review, Crit. Rev. Env. Sci. Technol. 39 (2009) 433–477.
[20] A. Korchef, H. Saidou, M.B. Amor, Phosphate recovery through struvite precipitation by CO2 removal: Effect of magnesium, phosphate and ammonium concentrations, J. Hazard. Mater. 186 (2011) 602–613.
[21] I. Stratful, M.D. Scrimshaw, J.N. Lester, Conditions influencing the precipitation of magnesium ammonium phosphate, Water Res. 35 (2001) 4191–4199.
[22] T. Zhang, L. Ding, H. Ren, Pretreatment of ammonium removal from landfill leachate by chemical precipitation, J. Hazard. Mater. 166 (2009) 911–915.
[23] A.A. Rouff, Temperature-dependent phosphorus precipitation and chromium removal from struvite-saturated solutions, J. Colloid Interface Sci. 392 (2013) 343–348.
[24] J.C. Warmadewanthi, Recovery of phosphate and ammonium as struvite from semiconductor wastewater, Sep. Purif. Technol. 64 (2009) 368–373.
[25] S. Uludag-Demirer, G.N. Demirer, S. Chen, Ammonia removal from anaerobically digested dairy manure by struvite precipitation, Process Biochem. 40 (2005) 3667–3674.
[26] W. Moerman, M. Carballa, A. Vandekerckhove, D. Derycke, W. Verstraete, Phosphate removal in agro-industry: Pilot- and full-scale operational considerations of struvite crystallization, Water Res. 43 (2009) 1887–1892.
[27] S.-H. Lee, B.-H. Yoo, S.-K. Kim, S.J. Lim, J.Y. Kim, T.-H. Kim, Enhancement of struvite purity by re-dissolution of calcium ions in synthetic wastewaters, J. Hazard. Mater. 261 (2013) 29–37.
[28] K.S. Le Corre, E. Valsami-Jones, P. Hobbs, S.A. Parsons, Impact of calcium on struvite crystal size, shape and purity, J. Cryst. Growth 283 (2005) 514–522.
[29] S.A. Parsons, F. Wall, J. Doyle, K. Oldring, J. Churchley, Assesing the potential for struvite recovery at sewage treatment works, Environ. Technol. 22 (2001) 1279–1286.
[30] P.G. Koutsoukos, A.N. Kofina, P.G. Klepetsanis, Exploration of alternatives for phosphorus recovery from wastewater by crystallization, in: WASIC workshop, Istanbul, 2003.
[31] I. Halikia, P. Neou-Syngouna, D. Kolitsa, Isothermal kinetic analysis of the thermal decomposition of magnesium hydroxide using thermogravimetric data, Thermochim. Acta 320 (1998) 75–88.
[32] C. Rodriguez-Navarro, E. Ruiz-Agudo, A. Luque, A. Rodriguez-Navarro, M. Ortega-Huertas, Thermal decomposition of calcite: Mechanisms of formation and textural evolution of CaO nanocrystals, Am. Mineral. 94 (2009) 578–593.
[33] Y. Jaffer, T.A. Clark, P. Pearce, S.A. Parsons, Potential phosphorus recovery by struvite formation, Water Res. 36 (2002) 1834–1842.
[34] J.D. Doyle, S.A. Parsons, Struvite formation, control and recovery, Water Res. 36 (2002) 3925–3940.
[35] D. Crutchik, J.M. Garrido, Struvite crystallization versus amorphous magnesium and calcium phosphate precipitation during the treatment of a saline industrial wastewater, Water Sci. Technol. 64 (2011) 2460–2467.
[36] M.S. Rahaman, N. Ellis, D.S. Mavinic, Effects of various process parameters on struvite precipitation kinetics and subsequent determination of rate constants, Water Sci. Technol. 57 (2008) 647–654.